Available online at www.sciencedirect.com
SCIENCE DIRECT®
ELSEVIER
Journal of Magnetism and Magnetic Materials 293 (2005) 265–270
Journal of magnetism and magnetic materials
www.elsevier.com/locate/jmmm

Synthesis of magnetoliposomes with monodisperse iron oxide nanocrystal cores for hyperthermia

Marcela Gonzales, Kannan M. Krishnan*

Department of Materials Science and Engineering, University of Washington, 323 Roberts Hall, Box 352120, Seattle, WA 98195-2120, USA

Available online 3 March 2005

Abstract

Heating rates generated by superparamagnetic particles deteriorate quickly with particle polydispersity. We prepared highly uniform, monodisperse, single-crystal magnetite nanoparticles of tailorable size via organometallic decomposition. As-synthesized nanocrystals were coated with phospholipids to form biocompatible magnetoliposomes. Modeling of AC-magnetic field parameters indicates that 11 nm nanocrystals have maximum heating rates within the biologically safe frequency range.

Keywords: Magnetic hyperthermia; Lipid bilayer; Magnetite; Nanoparticles; Superparamagnetic; $Fe(CO)_5$; Magnetoliposomes

1. Introduction

Hyperthermia, or the controlled heating of tissue to promote cell necrosis, with magnetic nanoparticles has been shown to be a powerful cancer treatment [1,2]. Magnetoliposomes (MLs), magnetic nanoparticles coated in a lipid bilayer, provide a highly flexible system for biocompatibility, chemical functionality and drug delivery resulting in a synergistic treatment strategy [3,4]. Both hydrophobic and hydrophilic drugs can be delivered with magnetoliposomes via lipid mediated exchange between the MLs and the cell membrane [5–7]. Magnetoliposomes are particularly useful for hyperthermia because lipid bilayer properties are highly dependent on temperature, allowing for the design of bilayer temperature response [8].

Magnetite is an ideal candidate material for the core of MLs. As an oxide, it is relatively stable in air and water and documented to be biocompatible [9,10]. Magnetite is ferrimagnetic, hence has a lower stray magnetic field intensity as compared to ferromagnetic materials. This lower field is beneficial because it minimizes the potential health risks posed by weak magnetic fields [11–14]. Additionally, when used for

*Corresponding author. Tel.: +1 206 543 2814; fax: +1 206 543 3100.
E-mail address: kannanmk@u.washington.edu (K.M. Krishnan).

0304-8853/$ - see front matter © 2005 Elsevier B.V. All rights reserved.
doi:10.1016/j.jmmm.2005.02.020

hyperthermia, ferrimagnetic materials have a lower chance of agglomeration due to magnetostatic interactions than ferromagnetic materials [15].

In order to generate the maximum heat for minimum ML dosage, it is critical to control the properties of the nanoparticle core and the ML surface modification. Heat generation by superparamagnetic particles is dependent on particle size (magnetic core and hydrodynamic), crystallinity and shape and particle polydispersity.

We have prepared highly uniform, monodisperse magnetite nanocrystals (NCs) of tailorable size (4–11 nm). A lipid surfactant coats the NCs during synthesis, plays a key role during nucleation and growth and influences the resulting NC geometry. As-synthesized NCs are initially hydrophobic. However, coating the NCs with a second lipid layer is an effective route to make them hydrophilic.

2. Synthesis and formation of MLs

Surfactant-coated magnetite NCs were synthesized by injection of an organometallic precursor into a surfactant-mediated solvent [16]. Octyl ether 99%, trimethylamine N-oxide, iron pentacarbonyl, oleic acid and chloroform were purchased from Aldrich. 1,2-Dipalmitoyl-sn-Glycero-3-Phosphocholine (DPPC) was purchased from Avanti Polar Lipids.

Particle size is dependent on the molar ratio of oleic acid to iron pentacarbonyl initially present in the synthesis; 1:1, 2:1 or 3:1. To prepare the magnetite NCs, oleic acid in 10 mL octyl ether was heated to 100 °C. Iron pentacarbonyl was injected into the hot solution and allowed to reflux at 283 °C. Nucleation was evident by a sharp darkening of the solution over a 30 s period. After nucleation, the solution was allowed to reflux for an additional 1.5 h. The solution was cooled to room temperature and trimethylamine N-oxide was added. The temperature of the solution was increased to 130 °C and heated for 2 h during which time the color of the solution turned from black to red. Afterwards, the temperature was increased and allowed to reflux for 1 h during which time the color of the solution turned black. The solution was cooled to room temperature, washed with ethanol and a black precipitate was magnetically separated from the solution.

Washed NCs were redispersed in chloroform, sonicated for 5 min, and DPPC in chloroform added. The chloroform was evaporated under a gentle stream of Ar forming a lipid/nanoparticle cake. Residual solvent was removed in a vacuum chamber. Phosphate buffer solution (10 × concentrate) was added to the cake to rehydrate the lipids for 2 h in an argon environment. The temperature of the solution was increased to approximately 50 °C in a water bath and sonicated for 30 min to produce the coated magnetoliposomes.

3. Structure and magnetic characterization

Nanoparticle cores and magnetoliposomes were characterized by transmission electron microscopy (TEM) and X-ray diffraction (XRD). TEM micrographs were obtained on a Phillips CM 100 microscope. XRD patterns were obtained with a Rigaku high brilliance diffractometer with a rotating anode and Cu $K_{\alpha;}$ radiation source ($\lambda = 0.15418$ nm). The average diameter of NCs was obtained with image analysis of TEM micrographs and from XRD peak broadening. Magnetoliposomes were imaged in TEM after staining with 1% uranyl acetate solution. Magnetic characterization was performed with a Quantum Design MPMS-5S Superconducting Quantum Interference Device (SQUID) magnetometer. AC susceptibility measurements as a function of temperature were performed with a heating rate of 1.5 K/min and field amplitude of 1 G at a frequency of 1000 Hz.

4. Results

The particle size can be controlled from 4 nm for a 1:1 synthesis, 7 nm for a 2:1 synthesis and 11 nm for a 3:1 synthesis. Visual inspection of TEM micrographs, in Fig. 1, shows that NCs are uniform in shape with slight faceting consistent with single crystal morphology. Analysis of TEM

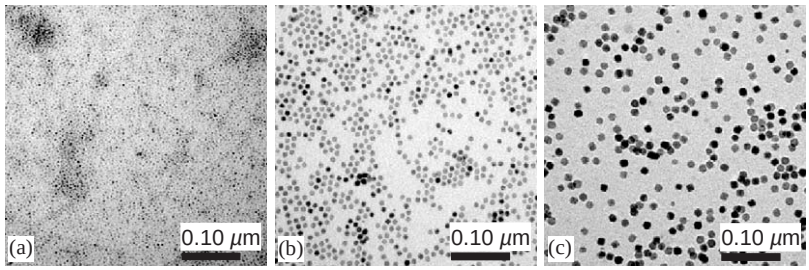

Fig. 1. TEM micrographs of magnetite NCs with diameters of (a) 4 nm (b) 7 nm and (c) 11 nm.

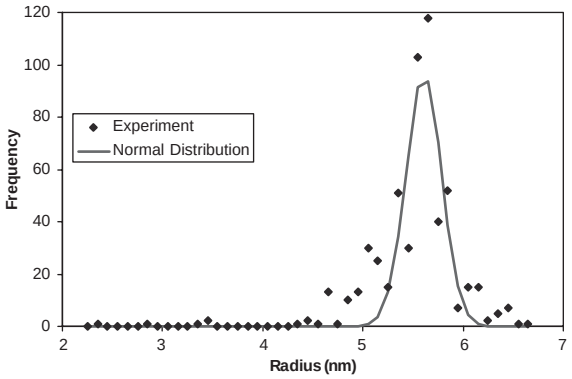

Fig. 2. Histogram of 11 nm magnetite NCs from digital analysis of TEM micrograph.

micrographs for NCs from a 3:1 synthesis with image analysis software (Fig. 2) resulted in an average particle diameter of 11.2 nm with a standard deviation of 0.18 nm. In Fig. 3, the XRD powder diffraction pattern illustrates the high crystallinity of the NCs. Peaks match very well with the Fe_3O_4 reflections. Analysis of XRD peak broadening data yields an average particle diameter of 11 ± 1 nm which correlates with the value obtained with TEM image analysis, further indicating single crystal nanoparticles. Visual inspection of ML from TEM micrographs, in Fig. 4, show many singly coated NC cores in a lipid bilayer, although some clusters of NCs were also seen.

Zero-field-cooled (ZFC) magnetization, field-cooled (FC) magnetization measurements and AC susceptibility as a function of temperature were performed on 7 nm NCs in powder form on the SQUID. Measurements, as seen in Fig. 5, revealed that the maximum of the imaginary component of the susceptibility occurred at a temperature of 50 K for a frequency of 1000 Hz.

5. Discussion

Particle size is highly dependent on the molar ratio of oleic acid to iron pentacarbonyl during synthesis. Increasing the concentration of the surfactant increases the energy barrier for nucleation, thus delaying the onset of nucleation and decreasing the number of nucleation events that occur, yielding a larger particle diameter. DPPC was chosen as the outer lipid layer based on its excellent biocompatibility [17] and ability to form small liposomes due to the ratio of head group size to hydrocarbon tail [18]. Formation of the magnetoliposomes is highly dependent on drying conditions. Dilute concentrations of NP yield the best lipid/NP cakes. Yield may be increase by removing the chloroform in a rotary evaporator.

To determine whether our NCs will have sufficient heating rates, we consider the guiding equations for hyperthermia. Temperature rise for a monodispersion of ferrofluid is given by $\Delta T = P\Delta t/c$, where c is the ferrofluid specific heat calculated as the volume average of the solid and liquid constituents, Δt is the duration of heating and P is the volumetric power dissipation given by

$$P = \mu_o \pi \chi'' f H_o^2, \quad (1)$$

where f is the frequency of the AC-field, $\mu_o = 4\pi \times 10^{-7}$ (T m A^{-1}) is the permeability of free space, χ'' is the imaginary component of the

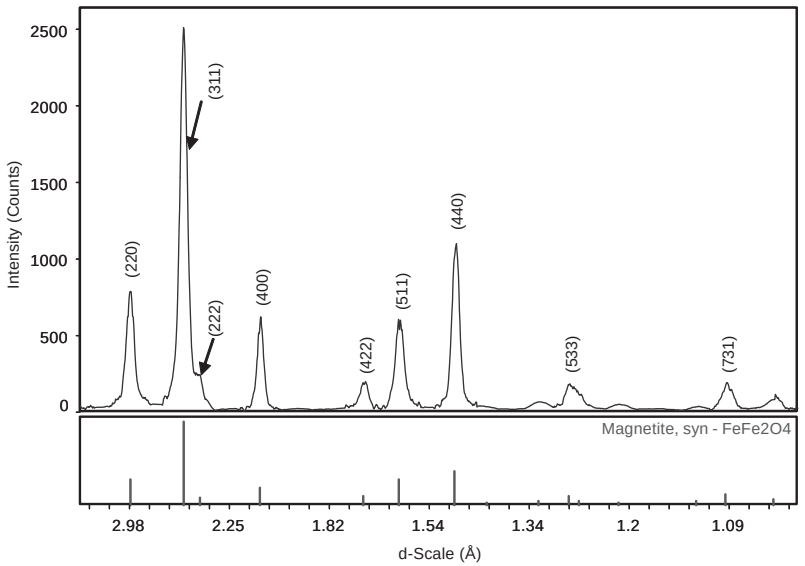

Fig. 3. XRD pattern of 11 nm magnetite NCs.

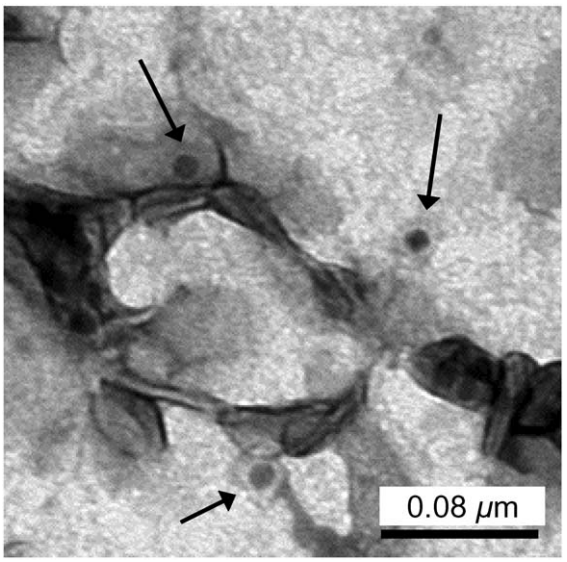

Fig. 4. TEM micrograph of ML with 1% UA stain.

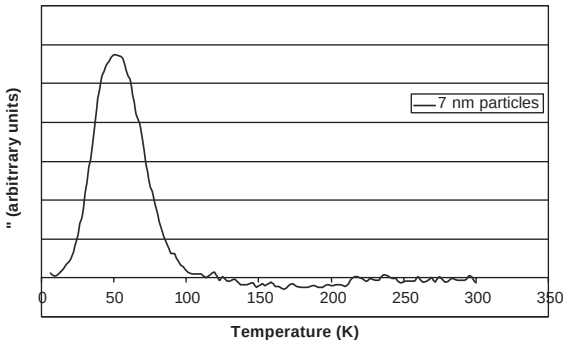

Fig. 5. Complex susceptibility as a function of temperature for 7 nm magnetite NCs with $f = 1000$ Hz.

susceptibility and H_o is the amplitude of the magnetic field.

The material properties of the ferrofluid are contained in χ'':

$$\chi'' = \chi_o \frac{2\pi f\tau}{1+(2\pi f\tau)^2}. \quad (2)$$

The effective relaxation time τ is given by

$$\frac{1}{\tau} = \frac{1}{\tau_B} + \frac{1}{\tau_N}. \quad (3)$$

The Brownian relaxation time constant τ_B is dependent on the surface modification of the particles:

$$\tau_B = \frac{3\eta V_H}{k_B T}, \quad (4)$$

where η is the viscosity of the matrix fluid, V_H is the hydrodynamic volume of the particle (particle

core plus surface coating and any associated layer of fluid), k_B is the Boltzman constant ($1.38 \times 10^{-23}\,J\,K^{-1}$) and T is the absolute temperature.

The Néel relaxation time constant, τ_N is related to the magnetic properties of the particles:

$$\tau_N = \frac{\sqrt{\pi}}{2}\tau_o \frac{\exp(KV_M/k_BT)}{(KV_M/k_BT)^{1/2}}, \quad (5)$$

where the attempt time $\tau_o = 10^{-9}\,s$, K is the anisotropy constant which may contain magnetocrystalline or shape anisotropy contributions and V_M is the magnetic volume of the particle.

For biological applications we will be limited in our choice of f and H_o to a biologically safe range, i.e. $H_o f \leqslant 4 \times 10^8\,A/m \times s$ [19]. Initially, the temperature will be fixed at body temperature (37 °C) and will eventually increase to a target temperature of approximately 45 °C. As a first approximation, the viscosity of biological fluids can be given by the viscosity of water at 37 °C.

In order to maximize ΔT we must maximize χ''. Maximum χ'' will occur at a specific f and H_o for a given set of material properties of the ferrofluid: nanoparticle size, shape, crystallinity and surface coating. Careful control of these properties is of great concern; moreover heating rates are quickly degraded with increasing particle polydispersity creating a strong incentive to use highly monodispersed ferrofluids [20]. χ'' will have a maximum value when $2\pi f\tau = 1$. By measuring χ'' as a function of temperature, for a given frequency, we can determine the temperature at which χ'' is a maximum. For measurements taken with particles in powder form, $\tau = \tau_N$. If V_M is known, K for the particles can be determined. Using the calculated K, V_H and the viscosity of water at 37 °C, the frequency, f_{max}, at which χ'' is a maximum can be estimated for the particles in physiological conditions.

Using this model, the anisotropy constant was determined to be $6.0 \times 10^4\,J/m^3$ for the 7 nm NCs. Using this value for K and assuming the NCs are coated with a 5 nm lipid bilayer, we calculate a maximum χ'' at 58 GHz at 310 K. Assuming the same K for the 11 nm NCs, we calculate a maximum χ'' at 380 kHz at 310 K corresponding to a maximum value of 1 kA/m for H_o. Therefore, the 7 nm NCs would not be useful for hyperthermia, but it is feasible that the 11 nm NCs could generate high heating rates. The relationship between temperature and f_{max} is plotted in Fig. 6 for the 7 and 11 nm NCs with and without contributions from Brownian relaxation.

It is interesting to note that for these NCs, the addition of Brownian relaxation increases f_{max} for the 11 nm particles but not for the 7 nm particles. Increasing V_H had very little effect on f_{max}. Considering that the viscosity of tissue is higher than water, calculations made with higher values of viscosity shifts f_{max} to lower frequencies. For an accurate model, the viscosity of tissue as a function of temperature will have to be considered.

For hyperthermia, we would like to increase the heat of the tumor area to 42–46 °C, approximately 320 K. As the temperature increases, f_{max} will shift to higher values (i.e., for our 11 nm NCs from 380 kHz at 310 K to 490 kHz at 320 K). Fig. 7 demonstrates that as temperature increases, for a

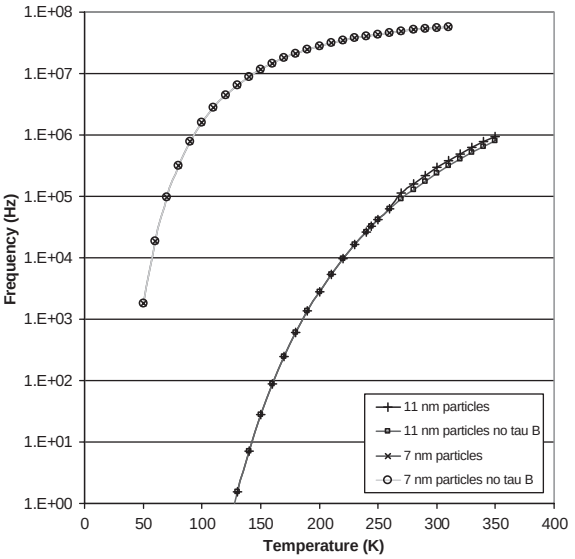

Fig. 6. Calculated frequency of maximum complex susceptibility as a function of temperature for 7 and 11 nm NCs with $K = 6 \times 10^4\,J/m^3$ with and without contribution from Brownian relaxation, τ_B. The figure shows that for 7 nm particles there is essentially no contribution from Brownian relaxation. For 11 nm particles, Brownian relaxation shifts f_{max} to larger values after 270 K.

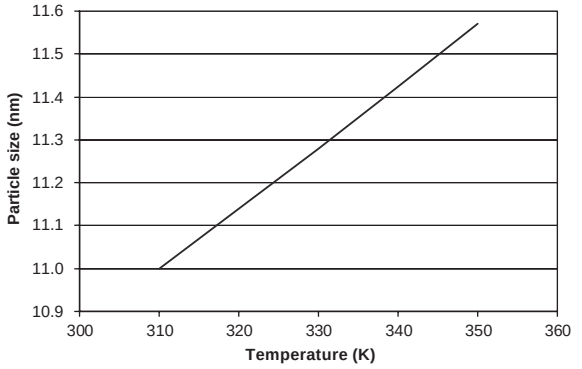

Fig. 7. Calculated particle size with maximum heating at $f = 380\,\mathrm{kHz}$ as a function of temperature.

given frequency, maximum heating will occur for NCs with larger diameters. Therefore for continued heating, either the frequency will have to increase with temperature or, for a given frequency, particle size distribution can be tailored to maintain heating.

6. Conclusions

We present the synthesis of magnetite nanocrystals which due to their uniformity and monodispersity appear ideal for hyperthermia applications. A lipid surfactant mediates the particle geometry and facilitates the formation of a lipid bilayer on the surface to form magnetoliposomes. Magnetic calculations indicate that for our size regime of NCs, most of the heating results from Néel relaxation, with V_H having little effect on the frequency at which maximum complex susceptibility occurs. We believe that our 11 nm NCs will have maximum heating rates within the biologically acceptable range.

Acknowledgements

The authors would like to thank Michael Beerman for insightful conversations and Dr. Alec Pakhomov for magnetic measurements. Funding provided by the Campbell Endowment and the National Physical Science Consortium.

References

[1] A. Jordan, P. Wust, R. Scholz, et al., in: U. Häfeli, W. Schütt, J. Teller, M. Zborowski (Eds.), Scientific and Clinical Applications of Magnetic Carriers, Plenum Press, New York, 1997.
[2] R. Hergt, W. Andrä, C.G. d'Ambly, et al., IEEE Trans. Magn. 34 (1998) 3745.
[3] M. De Cuyper, P. Müller, H. Lueken, M. Hodenius, J. Phys.: Condens. Mat. 15 (2003) S1425.
[4] M. De Cuyper, M. Joniau, Eur. Biophys. J. 15 (1988) 311.
[5] A.S. Ulrich, Biosci. Rep. 22 (2002) 129.
[6] F. Jähnig, Biophys. J. 46 (1984) 687.
[7] J. Hernandez-Borrell, F. Mas, J. Puy, Biophys. Chem. 36 (1990) 47.
[8] M. Babincová, P. Čičmanec, V. Altanerová, et al., Bioelectrochem. 55 (2002) 17.
[9] R. Weissleder, D.D. Stark, B.L. Engelstad, et al., Am. J. Roentgenol. 152 (1989) 167.
[10] B.R. Bacon, D.D. Stark, C.H. Park, et al., J. Lab. Clin. Med. 110 (1987) 164.
[11] J. Dobson, Ann. N.Y. Acad. Sci. 1012 (2004) 1.
[12] C.R. Timmel, U. Till, B. Brocklehurst, Mol. Phys. 95 (1998) 71.
[13] J.C. Scaiano, S. Monahan, J. Renaud, Photochem. Photobiol. 65 (1997) 759.
[14] C.F. Chignell, R.H. Sik, Photochem. Photobiol. 68 (1998) 589.
[15] J. Connolly, T.G. St. Pierre, J. Magn. Magn. Mater. 225 (2001) 156.
[16] T. Hyeon, S.S. Lee, J. Park, et al., J. Am. Chem. Soc. 123 (2001) 12798.
[17] M. Malmsten, B. Lassen, Colloids and Surfaces B.: Biointerfaces 4 (1995) 173.
[18] J.N. Isrelachvili, Intermolecular and Surface Forces, second ed., Academic Press, San Diego, California, 1992.
[19] I.A. Brezovich, Med. Phys. Monograph 16 (1988) 82.
[20] R.E. Rosensweig, J. Magn. Magn. Mater. 252 (2002) 370.